



OPEN ACCESS

EDITED BY

Ramasamy Palaniappan,
Sree Balaji Medical College and Hospital,
India

REVIEWED BY

Katalin Szaszi,
St. Michael's Hospital, Canada
Ira Kurtz,
University of California, Los Angeles,
United States
Annarita Di Mise,
University of Bari Aldo Moro, Italy

*CORRESPONDENCE

J. G. Hoenderop,
✉ joost.hoenderop@radboudumc.nl

[†]These authors have contributed equally to this work and share first authorship

SPECIALTY SECTION

This article was submitted to Stem Cell Research, a section of the journal Frontiers in Cell and Developmental Biology

RECEIVED 01 November 2022

ACCEPTED 06 January 2023

PUBLISHED 25 January 2023

CITATION

Olde Hanhof CJA, Dilmen E, Yousef Yengej FA, Latta F, Ammerlaan CME, Schreurs J, Hooijmaijers L, Jansen J, Rookmaaker MB, Orhon I, Verhaar MC and Hoenderop JG (2023), Differentiated mouse kidney tubuloids as a novel *in vitro* model to study collecting duct physiology. *Front. Cell Dev. Biol.* 11:1086823. doi: 10.3389/fcell.2023.1086823

COPYRIGHT

© 2023 Olde Hanhof, Dilmen, Yousef Yengej, Latta, Ammerlaan, Schreurs, Hooijmaijers, Jansen, Rookmaaker, Orhon, Verhaar and Hoenderop. This is an open-access article distributed under the terms of the [Creative Commons Attribution License \(CC BY\)](https://creativecommons.org/licenses/by/4.0/). The use, distribution or reproduction in other forums is permitted, provided the original author(s) and the copyright owner(s) are credited and that the original publication in this journal is cited, in accordance with accepted academic practice. No use, distribution or reproduction is permitted which does not comply with these terms.

Differentiated mouse kidney tubuloids as a novel *in vitro* model to study collecting duct physiology

C. J. A. Olde Hanhof^{1†}, E. Dilmen^{1†}, F. A. Yousef Yengej^{2,3}, F. Latta¹, C. M. E. Ammerlaan^{2,3}, J. Schreurs¹, L. Hooijmaijers¹, J. Jansen^{4,5,6}, M. B. Rookmaaker³, I. Orhon¹, M. C. Verhaar³ and J. G. Hoenderop^{1*}

¹Department of Molecular Physiology, Radboud Institute for Molecular Life Sciences, Radboud University Medical Center, Nijmegen, Netherlands, ²Hubrecht Institute, Royal Netherlands Academy of Arts and Sciences, Utrecht, Netherlands, ³Department of Nephrology and Hypertension, University Medical Center Utrecht, Utrecht, Netherlands, ⁴Department of Pathology, Radboud Institute for Molecular Life Sciences, Radboud University Medical Center, Nijmegen, Netherlands, ⁵Department of Pediatric Nephrology, Radboud Institute for Molecular Life Sciences, Radboud University Medical Center, Amalia Children's Hospital, Nijmegen, Netherlands, ⁶Institute of Experimental Medicine and Systems Biology, Medical Faculty RWTH Aachen University, Aachen, Germany

Kidney tubuloids are cell models that are derived from human or mouse renal epithelial cells and show high similarities with their *in vivo* counterparts. Tubuloids grow polarized in 3D, allow for long-term expansion, and represent multiple segments of the nephron, as shown by their gene expression pattern. In addition, human tubuloids form tight, functional barriers and have been successfully used for drug testing. Our knowledge of mouse tubuloids, on the other hand, is only minimal. In this study, we further characterized mouse tubuloids and differentiated them towards the collecting duct, which led to a significant upregulation of collecting duct-specific mRNAs of genes and protein expression, including the water channel AQP2 and the sodium channel ENaC. Differentiation resulted in polarized expression of collecting duct water channels AQP2 and AQP3. Also, a physiological response to desmopressin and forskolin stimulation by translocation of AQP2 to the apical membrane was demonstrated. Furthermore, amiloride-sensitive ENaC-mediated sodium uptake was shown in differentiated tubuloids using radioactive tracer sodium. This study demonstrates that mouse tubuloids can be differentiated towards the collecting duct and exhibit collecting duct-specific function. This illustrates the potential use of mouse kidney tubuloids as novel *in vitro* models to study (patho)physiology of kidney diseases.

KEYWORDS

tubuloid, organoid, epithelial sodium transport, cell physiology, collecting duct, tubulopathy

Introduction

The kidneys maintain homeostasis of fluids and electrolytes, remove waste products from the blood and regulate blood acid-base balance (Alpern and Hebert, 2007). Kidneys are composed of multiple nephron segments: the proximal tubule (PT), the loop of Henle (LoH), distal convoluted tubule (DCT), connecting tubule (CNT) and finally the most distal part of the nephron, the collecting duct (CD) (Alpern and Hebert, 2007). The principal cells (PCs) of the CD perform final water reabsorption, whereas the intercalated cells (ICs) of the CD are important for maintaining blood acid-base homeostasis (Fushimi et al., 1993; Brown, 2003). PC water reabsorption is promoted by the hormone arginine vasopressin (AVP) (Fushimi et al., 1993; van Lieburg et al., 1995; Brown, 2003). AVP binds to the

vasopressin type-2 receptor (V2R), which promotes translocation of the water channel aquaporin 2 (AQP2) towards the apical membrane (Yamamoto et al., 1995; Sandoval et al., 2013; Jung and Kwon, 2019). Basolateral water extrusion is mediated by the AQP3 and AQP4 water channels (Ishibashi et al., 1994; Terris et al., 1995). PCs of the CD also mediate final kidney sodium (Na^+) reabsorption by the apically expressed amiloride-sensitive epithelial sodium channel (ENaC), a heteromultimeric channel that consists of three subunits, alpha, beta and gamma (Canessa et al., 1994; Bhalla and Hallows, 2008). Basolateral Na^+ excretion is mediated by the Na^+ /potassium (K^+)-ATPase (Doucet, 1988). Dysregulation of this CD electrolyte handling can lead to hereditary (e.g., nephrogenic diabetes insipidus, Liddle's syndrome and pseudohypoaldosteronism type 1a) or acquired diseases that show wasting of electrolytes and/or water (Geller et al., 2006; Enslow et al., 2019; Kavanagh and Uy, 2019; Downie et al., 2021).

Our current understanding of kidney (patho)physiology stems from detailed studies using (immortalized) cell models and/or animal models. It is evident that these cell models are often too simplistic to mimic the complex *in vivo* situation (Jensen and Teng, 2020). A major limitation of immortalized cell lines is their lack of a physiological expression profile of key kidney markers, since conventional immortalization induces cellular dedifferentiation (Jenkinson et al., 2012; Gartzke and Fricker, 2014; Ramboer et al., 2014; Van der Hauwaert et al., 2014; Labarca et al., 2015; Slusser et al., 2015; Yu et al., 2018). Primary kidney cells in culture can overcome this problem, but are known to lose expression of relevant proteins within days (Baer et al., 2006; Terryn et al., 2007; Van der Hauwaert et al., 2013). Although animal models such as mice do provide the context of the *in vivo* situation, they are often time consuming and expensive (Russell and Burch, 1959). Therefore, novel research models are needed to advance understanding of kidney (patho)physiology.

Recently, three-dimensional (3D) kidney organoid models have been developed that can be grown either from induced pluripotent stem cells (iPSCs), first described in 2014, or from adult stem/progenitor cells (ASPCs) as described by Schutgens et al. (2019) Clevers (2016). The directed differentiation of iPSC-derived organoids recapitulates nephrogenesis and produces multiple cell types that have similar maturity to the first or second trimester of the human fetal kidney (Takasato et al., 2015; Wu et al., 2018; Combes et al., 2019). ASPC-derived kidney organoids or tubuloids correspond with a more mature expression profile compared to iPSC-derived kidney organoids. Tubuloids are grown in a 3D environment from primary renal epithelial cells by inducing a dedifferentiated progenitor state through amplification of Wnt signaling and activation of receptor tyrosine kinases. ASPC-derived kidney organoids consist solely of polarized adult kidney tubular epithelium and are, therefore, also referred to as tubuloids (Schutgens et al., 2019). Schutgens et al. (2019) showed that tubuloids could be obtained from human and mouse primary kidney tissue and could be maintained in culture for at least 20 weekly passages while retaining genetic stability. Human tubuloids were shown to express markers of different nephron segments; predominantly the PT, limited expression of the LoH, DCT and the CD and absence of glomerular cells. Interestingly, growth factor withdrawal in tubuloids further enhanced expression of markers of the distal part of the nephron. The first proof of principle experiments confirmed that human tubuloids formed tight and intact barriers, could be used in an organ-on-a-chip

system, and contained functional transporters (P-glycoprotein) (Schutgens et al., 2019; Gijzen et al., 2021). Also, tubuloids have been used to generate a large biobank of kidney cancers and for nephrotoxicity screening (Calandrini et al., 2020; Schutgens et al., 2021; Wiraja et al., 2021). However, in contrast to the detailed reports of human tubuloids, our knowledge of mouse tubuloids is limited (Schutgens et al., 2019).

Here, we further characterize the mouse kidney tubuloid model and describe a protocol to differentiate tubuloids towards the CD. We then validate the mRNA and protein expression of multiple CD transporters/channels and assess functionality of the tubuloid model. A functional *in vitro* CD mouse model allows for detailed studies of kidney (patho)physiology and complements existing mouse models of, e.g., CD tubulopathies. In this study, mouse tubuloid CD differentiation resulted in significantly upregulated CD mRNA and proteins. Functional studies with CD-enriched tubuloids demonstrated amiloride-sensitive ENaC-mediated Na^+ uptake. Therefore, mouse kidney tubuloids are proposed as a novel model to study kidney CD physiology *in vitro*.

Materials and methods

Animals

Wild-type female C57BL/6 mice (*Mus musculus*) were kept at the animal facility of the Radboud University in Nijmegen. Animals were housed with six per cage under standard conditions with bedding in a temperature-controlled room with a 12-h light/dark cycle. Water and standard pellet chow were available *ad libitum* (Ssniff Spezialdiäten, Soest, Germany). Mice were sacrificed at the age of 24 days by cervical dislocation and their kidneys were harvested. The animal procedures were performed in accordance with the guidelines of the Animal Ethics Board of the Radboud University Nijmegen.

Mouse-derived tubuloid culture

Kidneys from 2 C57BL/6 mice (hereafter referred to as tubuloid line A and B) were digested by 1 $\mu\text{g}/\text{mL}$ collagenase (LS004194, Worthington) treatment for 1.5 h to obtain tubular fragments. Fragments were embedded in Cultrex reduced growth factor Basement Membrane Extract (BME) type 2 (3533-001-02, R&D Systems) and cultured in expansion medium (EM) consisting of basal medium (BM) (advanced DMEM/F12 (12634028, Thermo Fisher Scientific) supplemented with 1% (v/v) penicillin/streptomycin, 1% (v/v) HEPES (H3375, Sigma-Aldrich) and 1% (v/v) GlutaMAX (35050038, Thermo Fisher Scientific) with 1.5% (v/v) B-27 supplement (17504044, Gibco), 1% (v/v) RSP03-Fc fusion protein conditioned medium (R001, U-Protein Express BV), N-acetylcysteine (1 mM, A7250, Sigma-Aldrich), FGF-10 (100 ng/mL, 100-26, Peprotech), A 83-01 (5 μM , SML0788, Sigma-Aldrich), EGF (50 ng/mL, AF-100-15, Peprotech) and Y-27632 (10 μM , HY-10583, MedChem Express) (Table 1). Tubuloids were kept at 37°C with 5% CO_2 and medium was changed three times per week. Tubuloids were passaged 1:2 to 1:3 weekly by mechanical shearing with a flame-polished pipette (Gijzen et al., 2021). Tubuloid CD differentiation medium (CM) consisted of BM supplemented with forskolin (10 μM , F6886, Merck), A 83-01 (5 μM , SML0788, Merck) and PD0325901 (1 μM , S1036, Pfizer) (Table 1). Tubuloid desmopressin (DDAVP) stimulation medium

TABLE 1 Composition of the media used.

Medium	Components
Growth factor withdrawal medium (BM)	Advanced DMEM/F12 with penicillin/streptomycin (1% v/v), HEPES (1% v/v), and GlutaMAX (1% v/v)
Expansion medium (EM)	BM with B-27 supplement (1.5% v/v), RSPO3 conditioned medium (1% v/v), N-acetylcysteine (1 mM), FGF-10 (100 ng/mL), A 83-01 (5 μ M), EGF (50 ng/mL), and Y-27632 (10 μ M)
CD differentiation medium (CM)	BM with forskolin (10 μ M), A 83-01 (5 μ M), and PD0325901 (1 μ M)
Desmopressin (DDAVP) stimulation medium	BM with DDAVP (10 nM), A 83-01 (5 μ M), and PD0325901 (1 μ M)
CD stimulation medium	BM with forskolin (10 μ M), A 83-01 (5 μ M), and fludrocortisone acetate (10 μ M)

consisted of BM supplemented with DDAVP (10 nM, V1005, Sigma-Aldrich), A 83-01 (5 μ M) and PD0325901 (1 μ M) (Table 1).

RNA isolation, cDNA generation and real time quantitative PCR (RT-qPCR)

Total RNA was isolated from tubuloids using the Nucleospin RNA XS kit (740902.50, Macherey-Nagel) according to the manufacturer's instructions. To obtain cDNA, the RNA was subjected to reverse transcription using M-MLV according to manufacturer's instructions (28025013, Thermo Fisher Scientific). Subsequently, the diluted cDNA was used to determine gene expression levels using the CF96 real time PCR detection system (185-4095-IVD, Bio-Rad). PCR program was as follows: 1) 7 min 95°C; 2) 15 s 95°C (denaturation); 3) 1 min 60°C; 4) back to 2) for 39 cycles; 5) 10 s 95°C; 6) 5 s/0.5°C 60°C–95°C. All gene expression levels were normalized to *Hprt* housekeeping gene. The primer sequences can be found in Table 2. Relative

expression values were determined using the $\Delta\Delta$ CT method, where the control condition was arbitrarily set at 1.

Western blot

Tubuloid samples were lysed with Triton lysis buffer (50 mM Tris-HCl pH 7.5, 1 mM EGTA, 1 mM EDTA, 1% (v/v) Triton X-100 (X100, Sigma-Aldrich), 10 mM sodium glycerophosphate, 1 mM sodium orthovanadate, 50 mM sodium fluoride, 10 mM sodium pyrophosphate, 270 mM sucrose and 150 mM sodium chloride) supplemented with protease inhibitors (1 μ g/mL pepstatin (0219536825, MP Biochemicals), 5 μ g/mL leupeptin (0215155380, MP Biochemicals), 1 μ M phenylmethanesulfonyl fluoride (P7626, Sigma-Aldrich) and 1 μ g/mL aprotinin (1371803, Serva Electrophoresis)) and 0.1% (v/v) beta-mercaptoethanol (M6250, Sigma-Aldrich). Subsequently, proteins were denatured in Laemmli sample buffer (2% (v/v) SDS (205-788-1, Serva), 0.01% (w/v) bromophenol blue (161-0404, Bio-Rad), 6% (v/v) glycerol (800688, MP Biochemicals), and 60 mM Tris-HCl/pH 6.8) containing 100 mM of DTT (04856126, MP Biochemicals) for 30 min at 37°C. Protein samples were run on 10% (v/v) (for AQP2) and 8% (v/v) (for ENaC) SDS-PAGE gel and transferred to a methanol-activated polyvinylidene difluoride membrane (IPVH00010, Millipore). The immunoblots were then blocked rotating in 5% (w/v) non-fat dried milk (NFD) in TBS-T (0.3% (v/v) Tween (0777, VWR Chemicals), 10 mM Tris pH 8, and 150 mM NaCl) for 45 min. Following this, blots were incubated rotating in primary antibodies (Table 3) diluted in 1% (w/v) NFD in TBS-T overnight at 4°C. Membranes were washed four times in TBS-T, followed by incubation while rolling with secondary HRP-conjugated antibodies diluted in 1% (w/v) NFD in TBS-T for 1 h at 4°C. The blots were visualised using the ImageQuant LAS 4000 (GE Healthcare) after applying SuperSignal West Pico PLUS Chemiluminescent Substrate (34580, Thermo Fisher Scientific).

TABLE 2 Primers.

Target gene	Forward (5'-3')	Reverse (5'-3')
<i>Hprt</i>	TTGCTGACCTGCTGGATTAC	AGTTGAGAGATCATCTCCAC
<i>Aqp2</i>	CTTTGCCCTCCACTGATGAGC	GGAGCGGGCTGGATTCAT
<i>Aqp3</i>	TTTGACCTCGCCTCTTCAC	TGAGCTGGTACACGAAGACA
<i>Scnn1a</i>	CATGCCTGGAGTCAACAATG	CCATAAAAGCAGGCTCATCC
<i>Scnn1g</i>	TGACCTGCTTCTTCGATGGG	TTGCAGACCATACTCACTGCC
<i>Avpr2</i>	CTCATCATCAGCCACCACAC	GGAGAGCTAGGGGACGAAAG
<i>Anpep</i>	ACCCCAACAACCTCATAGCT	ACTCAGTCATGGTGCAGGAA
<i>Umod</i>	ACTGCACCGATCCTAGFTCC	CACTCCAGCCTGTACTCCAA
<i>Pvalb</i>	GACGGCAAGATTGGGGTTG	ACTGAGATGGGGCGTTGG
<i>Calb1</i>	GACGGAAGTGGTTACCTGGA	ATTTCCGGTGATAGCTCCAA
<i>Slc4a1</i>	TGATGTTTGCTCCGTTCTG	AGCCCTTGATCATCTTCCGT
<i>Slc14a2</i>	GGACCTGAGTGACTGGCTATTT	ATCTCCTCAGGGGGTGGTG

TABLE 3 Antibodies/stains.

Antibody/stain	Origin	Dilution	Manufacturer
Alexa Fluor 488/594-conjugated antibodies	Goat	IHC 1:300	Thermo Fisher Scientific
AQP2	Guinea Pig	IHC 1:50	Homemade antibody Deen et al. (1994)
		WB 1:1,000	
AQP3	Rabbit	IHC 1:50 + TSA	Homemade antibody van Balkom et al. (2003)
Beta-actin	Mouse	WB 1:10,000	5441, Sigma Aldrich
Biotin-conjugated antibody	Goat	IHC 1:2,000	4050-08, Southern Biotech
DAPI		IHC 12.5 µg/mL	D1306, Invitrogen
E-cadherin	Rat	IHC 1:50	14-3249-82, Invitrogen
Alpha subunit of ENaC	Rabbit	WB 1:1,000	SPC-403D, StressMarq
Gamma subunit of ENaC	Rabbit	WB 1:1,000	Homemade antibody Masilamani et al. (1999)
Na ⁺ /K ⁺ -ATPase	Rabbit	IHC 1:200	Kind gift from Prof. Koenderink, Homemade antibody Koenderink et al. (2003)
PO-conjugated anti rabbit	Goat	WB 1:10,000	A4914, Sigma Aldrich
PO-conjugated anti human/rat/rabbit/mouse/guinea pig	Mouse	WB 1:10,000	A5441, Sigma Aldrich
ZO-1	Mouse	IHC 1:50	339100, Invitrogen

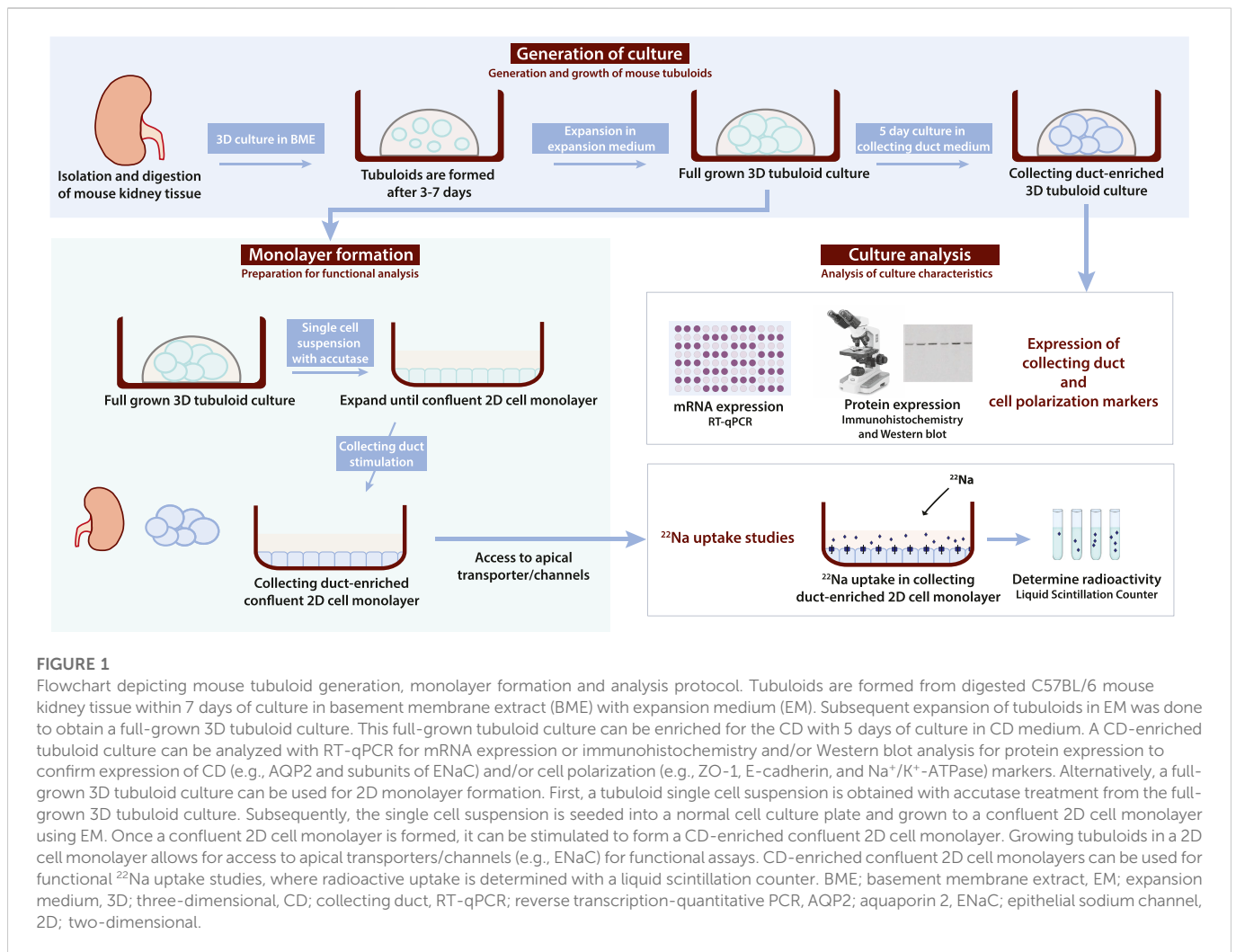
Immunohistochemistry (IHC) of 3D tubuloids

Tubuloids were fixated in 4% (w/v) formalin (4078-9001, KLINIPATH) for 15 min. Next, the tubuloids were collected and embedded in a cytoagar with 2.25% (w/v) agar (1.800.854.0530, MP Biomedicals) in PBS for 10 min at 4°C. Tubuloids were transferred to an embedding cassette and paraffinized. Subsequently, 5 µm slices were prepared using a paraffin microtome and mounted on FLEX IHC Microscope Slides (Dako, Agilent Technologies). For IHC, tubuloid slices were deparaffinized with 2 × 5 min of incubations in xylene (4055-9010, KLINIPATH) followed by rehydration by dipping in a series of 100%–50% ethanol and finally demi water. Next, target retrieval was performed by boiling in citrate buffer (10 mM sodium citrate, with pH set to 6.0 with citric acid) for 15 min followed by cooling for 30 min at RT and 30 min at 4°C. The slides were then permeabilized for 30 min in TN-buffer (0.15 M sodium chloride, 0.1 M Tris-HCl, pH 7.6) with 0.1% (v/v) Triton X-100 and blocked for 30 min using TN with 0.5% (w/v) blocking reagent from the TSA fluorescein kit (NEL701A001KT, PerkinElmer). The slides with the primary antibodies (Table 3) were incubated overnight at 4°C. Subsequently, slides were washed 3 × 5 min in TN buffer with 0.05% (v/v) Tween 20, followed by incubation with secondary antibodies and DAPI (Table 3). For the AQP3 antibody, TSA amplification was performed as follows. After permeabilization with Triton buffer, endogenous peroxidase activity was blocked with 0.3% (v/v) H₂O₂ (23622.298, VWR International) for 30 min and endogenous avidin/biotin binding sites were blocked (Avidin/Biotin Blocking kit (927301, BioLegend)) for 15 min each. After incubation with primary and secondary biotin-conjugated antibodies (Table 3), slices were incubated with streptavidin-HRP for 30 min followed by 7 min incubation with fluorescein tyramide (both TSA Fluorescein

System). After mounting with Fluoromount-G (00-4958-02 Thermo Fisher Scientific), images were acquired with laser scanning microscopy (LSM900, Zeiss) objective ×63 (NA 1.4) and processed with FIJI software (ImageJ) ([Schindelin et al., 2012](#)). To generate single images of whole tubuloids, multiple images were stitched together ([Preibisch et al., 2009](#)).

²²Na uptake experiments

Tubuloids were resuspended in accutase (A6964, Sigma-Aldrich) and incubated for 30 min at 37°C followed by shearing (15x) with a flame-polished pipette until a single cell suspension was reached. Subsequently, 60,000 cells per well were seeded on 24-well cell culture plates (3524, Corning) and grown in EM until confluent. Subsequently, tubuloid monolayers were cultured in CD stimulation medium consisting of BM supplemented with forskolin (10 µM, F6886, Merck), A 83-01 (5 µM, SML0788, Merck) and fludrocortisone acetate (10 µM, F0180000, Merck) for 5 days (Table 1). Before start of the experiment the tubuloids were pre-incubated for 30, 90 or 150 min with uptake buffer (70 mM Na⁺ D-gluconate, 2.5 mM K⁺ D-gluconate, 0.5 mM CaCl₂, 0.5 mM MgCl₂ and 2.5 mM HEPES, with pH set to 7.4 using Tris) and inhibitors. The inhibitors used for different conditions were ouabain (1 mM, 102541, MP Biomedicals), hydrochlorothiazide (0.1 mM, H4759, Sigma Aldrich), bumetanide (0.1 mM, B3023, Sigma Aldrich) and/or amiloride (0.1 mM, A7410, Sigma Aldrich) and/or dimethyl sulfoxide (DMSO) as vehicle control. Next, the buffers were replaced with buffers containing tracer ²²Na (U.S. Department of Energy Isotope Program) for 30 min of incubation at 37°C. Finally, the tubuloids were washed with ice-cold uptake buffer and lysed 15 min with 0.05% (w/v) SDS. The tracer ²²Na radioactivity was measured using a liquid scintillation counter (Hidex 300SL).



Statistical analysis

Statistical analysis was performed using One-Way ANOVA combined with Dunnett's multiple comparisons test or Two-Way ANOVA combined with Sidak or Tukey multiple comparisons test using Prism version 8 (Graphpad, United States). Error bars represent the mean \pm standard error of the mean (SEM) and the statistical significance was set at $*p < 0.05$.

Results

Tubuloids can be grown from adult mouse kidneys and differentiated towards CD phenotype

Kidney tubuloids were formed by digesting mouse kidneys from C57BL/6 mice and resuspending digested tissue in basement membrane extract (BME) for subsequent culture (Figure 1). Typically, the first tubuloids developed within 3–7 days of culture in expansion medium (EM) (Table 1) and could be further cultured for at least 10 weekly passages (Figures 1, 2A). With EM, we promoted canonical Wnt signalling, essential for kidney repair (Adams et al.,

2010), stimulated proliferation and survival of progenitor cells (Poladia et al., 2006), and inhibited anoikis of dissociated cells (Watanabe et al., 2007).

In this study, we applied the existing human tubuloid culture protocol to the mouse tubuloids and stimulated expression of CD mRNA and proteins (e.g., ENaC and AQP2) (Figure 1). We established a mouse CD-enriched 3D tubuloid culture by a 5-day culture of full-grown tubuloids in CM (Table 1). With CM, we stimulated the enzyme adenylate cyclase, the downstream mediator of AVP (Nielsen et al., 1995), inhibited the mitogen extracellular kinase (MEK1/2), a regulator of cell proliferation and differentiation (Kohno and Pouyssegur, 2006; Degirmenci et al., 2020), and inhibited the TGF- β receptors ALK4/5/7 that promote dedifferentiation and epithelial-to-mesenchymal transition (Tojo et al., 2005). Subsequently, the CD-enriched 3D tubuloid culture was analyzed for expression of CD (e.g., ENaC and AQP2) and cell polarization markers (i.e., ZO-1, E-cadherin and the Na⁺/K⁺-ATPase). Alternatively, the fully grown 3D tubuloid cultures could be formed into a single cell suspension, seeded as 2D cell monolayers, and expanded to a confluent 2D cell monolayer. After stimulation for the collecting duct, the CD-enriched 2D cell monolayers were used for functional ²²Na uptake experiments (Figure 1).

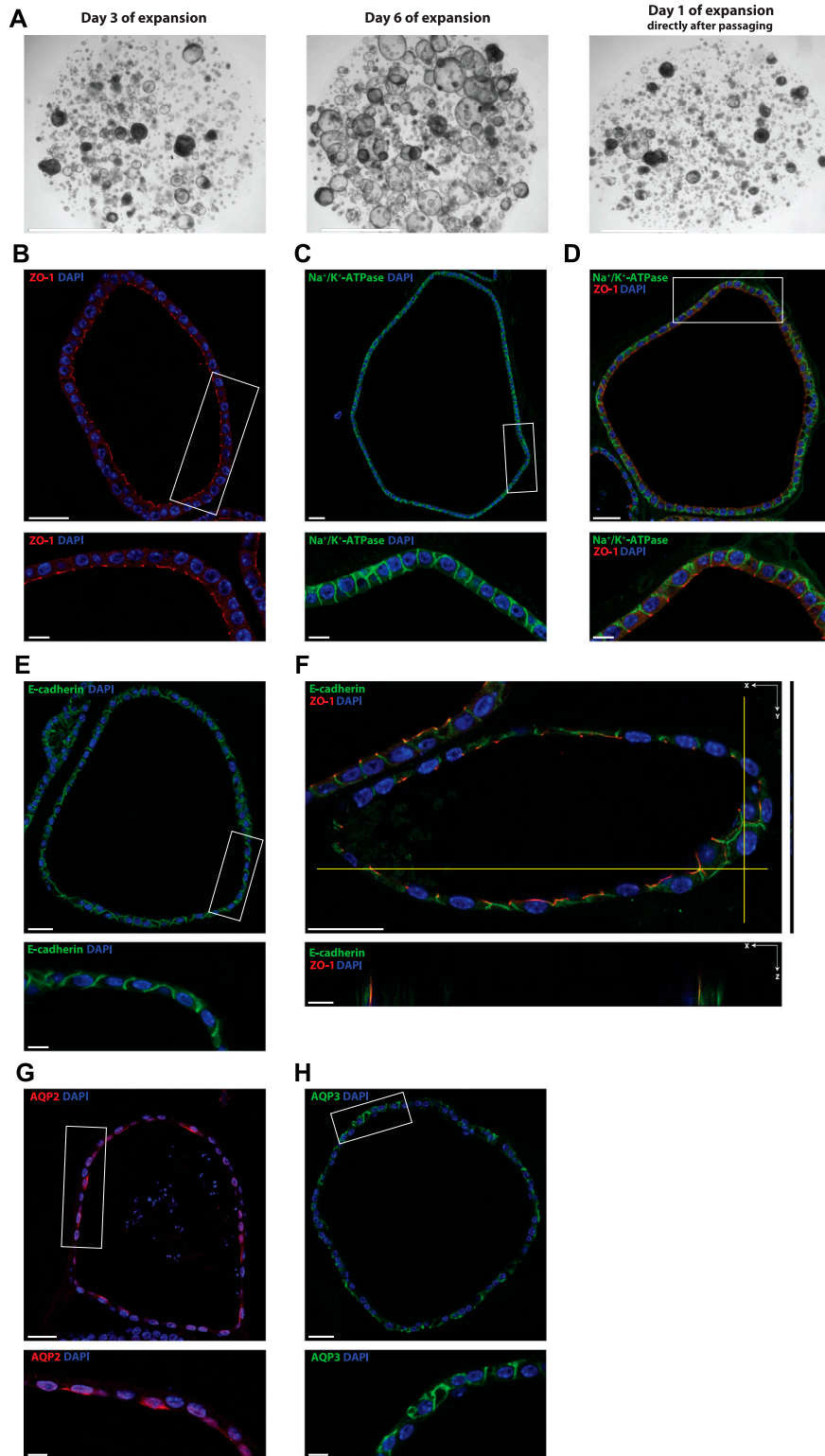


FIGURE 2

Mouse tubuloids enriched for the CD are polarized and express CD proteins (water channels AQP2/AQP3). Brightfield images of tubuloids growth after 3 and 6 days in culture with EM. Tubuloids were passaged after 7 days in culture, this is referred to as day 1 of expansion directly after passaging (A). Representative immunofluorescence pictures of CD-enriched mouse tubuloids (B–H). Expression of the apical tight junction protein ZO-1 (red) (B, D, F), basolateral Na⁺/K⁺-ATPase (green) (C, D) and lateral adherens junction protein E-cadherin (green) (E, F). Staining of CD proteins AQP2, apical water channel, (red) (G) and AQP3, basolateral water channel, (green) (H) after CD enrichment with CM, which includes forskolin. Inserts (white rectangle) are displayed directly below the main image (B–H). XZ direction of Z-stack of the costaining of ZO-1 and E-cadherin is displayed directly below the main image (F). Tubuloids were stained for nuclei (DAPI, blue) (B–H). Scale bars (A) 2 mm, (B–H) 30 μm and inserts/z-stack 10 μm. CD; collecting duct, EM; expansion medium, CM; collecting duct differentiation medium, ZO-1; zonula occludens 1, Na⁺; sodium, K⁺; potassium, AQP2/3; aquaporin 2/3.

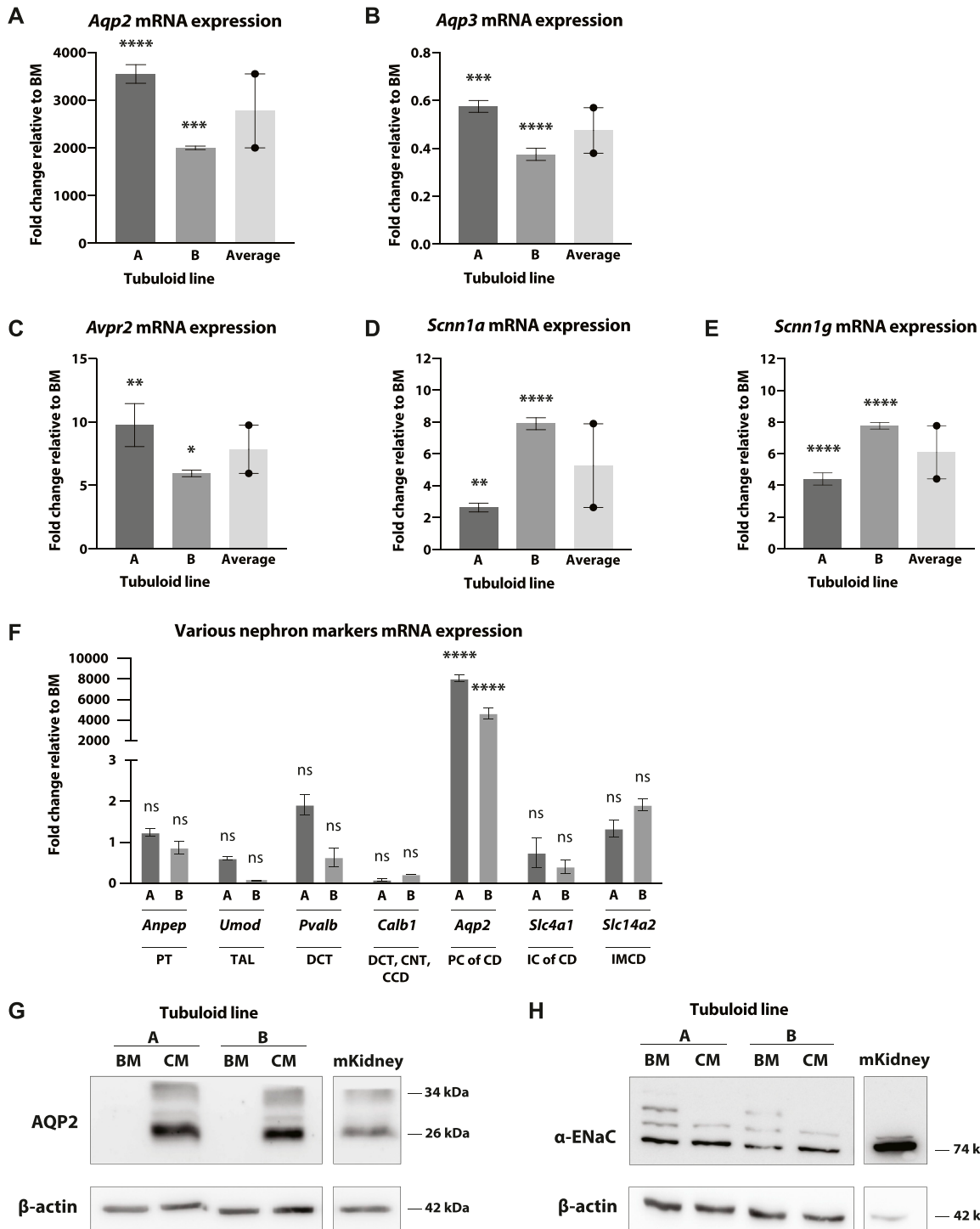


FIGURE 3 mRNA and protein expression of multiple CD transporters in CD-enriched mouse tubuloids. Fold change mRNA expression of tubuloid line A and B cultured in CD medium (CM) compared to basal medium (BM). mRNA expression of CD water transporters *Aqp2* (A) and *Aqp3* (B), the V2R (*Avpr2*) (C) and the alpha (D) and gamma (E) subunits of ENaC (*Scnn1a* and *Scnn1g*) in 2 tubuloid lines, (A, B), after culture in CM (N = 2-3 replicates). Average of the 2 tubuloid lines is included in all graphs (N = 2 duplicates). mRNA expression of *Anpep* (PT), *Umod* (TAL), *Pvalb* (DCT), *Calb1* (DCT/CNT/CCD), *Aqp2* (PC, CD), *Slc4a1* (IC, CD), and *Slc14a2* (IMCD) in 2 tubuloid lines, (A, B), after CM culture (N = 2/4 replicates) (F). Western blot of AQP2 (G) and the alpha subunit of ENaC (H) in the 2 tubuloid lines after culture with CM and BM. A sample from wild type mouse kidney cortex is included as control. ns, not significant; *p < 0.05, **; p < 0.01, ***; p < 0.001, ****; p < 0.0001. CD, collecting duct; AQP2/3, aquaporin 2/3; V2R, AVP receptor; ENaC, epithelial sodium channel; PT, proximal tubule; TAL, thick ascending limb of the loop of Henle; DCT, distal convoluted tubule; CNT, connecting tubule; CCD, cortical collecting duct; PC, principal cell; CD, collecting duct; IC, intercalating cell; IMCD, inner medullary collecting duct; CM, CD medium; BM, basal medium.

The morphology of a typical tubuloid culture immediately after passaging, at day 3 and at day 6 is depicted in [Figure 2A](#). CD-enriched tubuloids consisted of a polarized epithelium made up of a single cell layer as shown by expression of the apical zonula occludens 1 (ZO-1), a tight junction-associated protein, ([Figures 2B, D, F](#)), basolateral Na⁺/K⁺-ATPase ([Figures 2C, D](#)) and the lateral adherens junction protein E-cadherin ([Figures 2E, F](#)). Additionally, the XZ direction of the ZO-1 and E-cadherin costaining showed a partial overlap of these proteins, which confirms the correct localization of ZO-1, since it acts as a binding partner for both tight and adherens junctions ([Campbell et al., 2017](#)). Furthermore, immunofluorescence microscopy showed expression of CD-specific water channels AQP2 and 3 after culture in CM ([Figures 2G, H](#)). Specific localization of AQP2 to the apical membrane ([Figure 2G](#)) and AQP3 to the basolateral membrane ([Figure 2H](#)) further confirmed the polarized CD specificity and response to stimulation with forskolin.

Collecting-duct enriched mouse kidney tubuloids express water and sodium channels and respond to stimulation with desmopressin

The CD characteristics of mouse kidney tubuloids cultured in CM were further investigated with mRNA and protein expression analysis ([Figure 1](#)). Expression levels were compared to culture in simple growth factor withdrawal medium (BM) ([Table 1](#)), which, previously, has been shown to increase marker expression of the distal part of the nephron in human tubuloids ([Schutgens et al., 2019](#)). Mouse tubuloids differentiated with CM showed a significant increase in mRNA expression of the water channel AQP2 compared to BM for both tubuloid lines assessed (A and B) ([Figure 3A](#)). Importantly, tubuloid lines A and B were isolated from 2 different C57BL/6 mice. In addition, Western blot analysis showed clear expression of AQP2 after culturing in CM and complete absence of AQP2 using BM, confirming the CD identity of mouse kidney tubuloids cultured in CM ([Figure 3G](#)). Furthermore, mRNA expression analysis showed that the basolateral CD water channel AQP3 could be detected in both tubuloid lines, although expression was somewhat reduced in CM culture ([Figure 3B](#)). These quantitative mRNA expression data, together with the basolateral AQP3 staining in immunofluorescence microscopy ([Figure 2H](#)) confirm the expression of AQP3 in our culture. Water reabsorption mediated by AQP2 and AQP3 in the CD is promoted by the hormone AVP ([Brown, 2003](#)). CD-enriched mouse kidney tubuloids demonstrated clear upregulation of the V2R after culture in CD medium compared to BM in both tubuloid lines ([Figure 3C](#)).

Mouse tubuloids differentiated with CM expressed the CD-specific apical Na⁺ channel ENaC, demonstrating a CD enrichment. Quantitative mRNA expression by RT-PCR analysis indicated that both the alpha and gamma subunits of ENaC (*Scnn1a* and *Scnn1g*) were significantly increased in the 2 tubuloid lines after CM culture ([Figures 3D, E](#)). Protein expression of the alpha subunit of ENaC was confirmed with Western blot ([Figure 3H](#)). We observed relatively high baseline expression of alpha ENaC in BM culture ([Figure 3H](#)), compared to the other CD-marker AQP2.

Differentiation with CM led to an increase in markers of the CD and not of other nephron segments in both tubuloid lines. Also, we did not observe an increase in ICs of the CD or in PCs of the inner

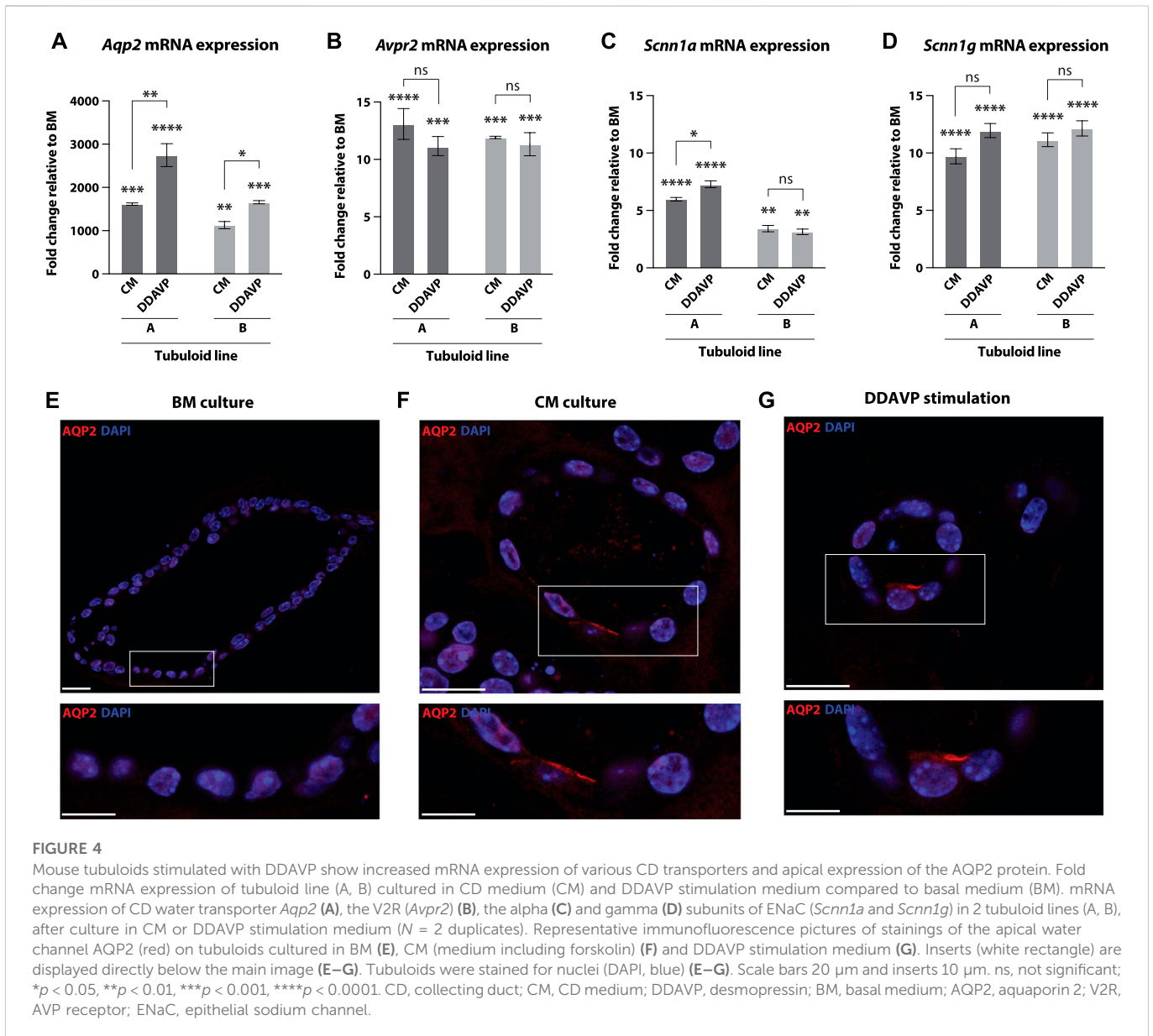
medullary collecting duct (IMCD). mRNA expression of *Anpep* (Aminopeptidase N, expressed in the PT), *Umod* (Uromodulin, expressed in the thick ascending limb of the LoH (TAL)), *Pvalb* (Parvalbumin, expressed in the DCT), *Calb1* (Calbindin D-28K, expressed in the DCT/CNT/cortical collecting duct (CCD)), *Slc4a1* (Anion exchanger 1, expressed in type A ICs, CD), and *Slc14a2* (Urea transporter A (UT-A), expressed in PCs of the IMCD) was not significantly increased after CM differentiation compared to BM ([Figure 3F](#)). Simultaneously, a significant increase in *Aqp2* mRNA expression was observed. These results, together with the absence of expression enrichment of Calbindin D-28K and UT-A, and enrichment of expression of the alpha and gamma subunit of ENaC ([Figures 3D, E](#)) suggests that the tubuloid differentiation is directed towards the outer medullary collecting duct (OMCD) rather than to other segments of the CD (CCD or IMCD).

Next, the tubuloids were stimulated with DDAVP, a synthetic variant of the hormone vasopressin, to verify that the V2R was physiologically functional in the tubuloid culture ([Ufer et al., 1995](#)) ([Table 1](#)). We observed a significant increase in mRNA expression of AQP2, the V2R, and the alpha and gamma subunits of ENaC after DDAVP stimulation compared to BM for both tubuloid lines ([Figures 4A–D](#)). mRNA expression of AQP2 was significantly increased after DDAVP stimulation compared to CM ([Figure 4A](#)), and one of the tubuloid lines also showed a significant increase of the alpha subunit of ENaC upon DDAVP stimulation ([Figure 4C](#)). Expression of the V2R and the gamma subunit of ENaC was not changed after DDAVP stimulation compared to CM ([Figures 4B, D](#)), thereby showing the similarities between the effect of DDAVP and forskolin (CM medium) ([Maric et al., 1998; Hasler et al., 2002](#)). Expression of AQP2 and apical localization after DDAVP stimulation was confirmed with immunofluorescence microscopy. The control BM culture showed an absence of AQP2 ([Figure 4E](#)), whereas the CM culture ([Figure 4F](#)) and DDAVP stimulation ([Figure 4G](#)) induced clear expression and apical localization of AQP2 as expected.

Mouse tubuloids enriched for the collecting duct show physiological ENaC-mediated Na⁺ uptake

After observing increased CD protein expression in the tubuloids that were differentiated with CM, we investigated whether these proteins were capable of Na⁺ uptake. Because mouse tubuloids in BME consist of polarized cell layers with an enclosed apical compartment facing the lumen ([Figures 2B, D, F](#)), we developed a tubuloid cell monolayer culture to gain access to the apical membrane for functional studies ([Figures 1, 5A](#)). Tubuloids were formed into a single cell suspension, seeded and grown into a confluent 2D cell monolayer, and stimulated to generate CD-enriched confluent 2D cell monolayers with access to apical transporters/channels. Here, ENaC function and activity was further stimulated with fludrocortisone ([Table 1](#)).

To determine the effect of CD stimulation with fludrocortisone in 2D and 3D tubuloids ([Figure 5A](#)), the expression of several markers of the distal parts of the nephron including α-ENaC (*Scnn1a*), NCC (*Slc12a3*, expressed in the DCT) and NKCC2 (*Slc12a1*, expressed in the TAL) was verified with reverse transcription-quantitative PCR. mRNA expression of the alpha subunit of ENaC was significantly increased similarly in both 2D and 3D CD stimulation compared to

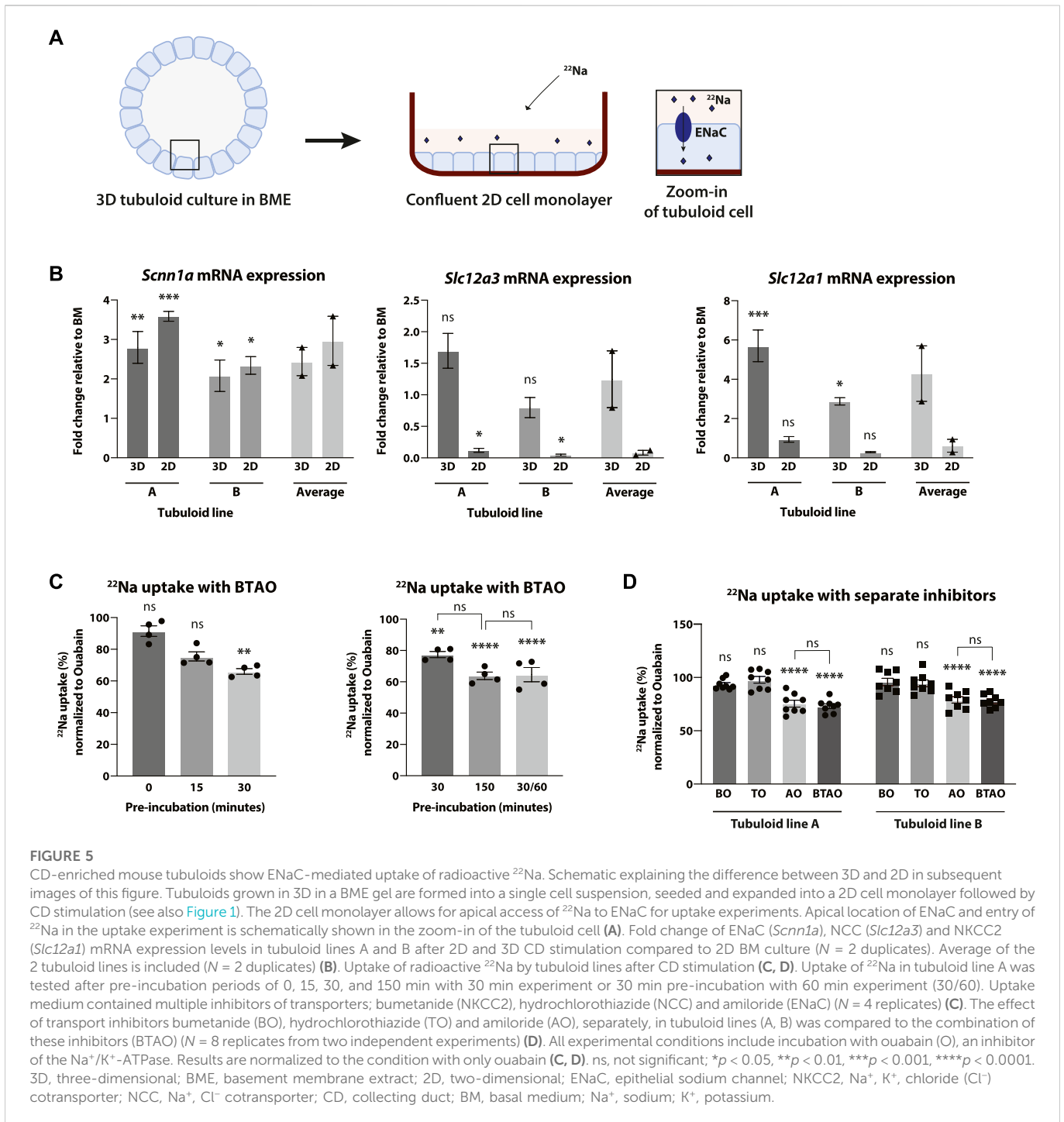


BM in both tubuloid lines. mRNA expression of NCC did not change significantly with CD stimulation in 3D, but was significantly downregulated in 2D. NKCC2 expression was significantly increased upon CD stimulation in 3D, but not in 2D (Figure 5B). Following these results, we concluded that 2D monolayer culture to access the apical compartment was also suitable for CD enrichment and, thus, for functional studies.

Next, functional uptake of the radioactive isotope ^{22}Na by the CD-enriched tubuloid monolayers was studied. The tubuloid monolayers were capable of ^{22}Na absorption as shown by the uptake of the radioactive ^{22}Na and the subsequent reduction in uptake after inhibition of the main Na^+ transporters of the distal part of the nephron (Figures 5C, D). The channels/transporters ENaC, NCC and NKCC2 were inhibited using amiloride (A), hydrochlorothiazide (T) and bumetanide (B), respectively. In addition, ouabain (O) was added in all conditions to prevent basolateral extrusion of ^{22}Na by the Na^+/K^+ -ATPase. The ^{22}Na uptake experiments included a pre-incubation with uptake buffer

including the inhibitors before the start of the experiment to allow the inhibitors to take effect. First, the optimal pre-incubation time was determined by performing ^{22}Na uptake with the cocktail of Na^+ transporter/channel inhibitors (BTAO). The decrease in uptake of ^{22}Na in response to apical inhibitors was significant after 30 and 150 min of pre-incubation, but not for 0 and 15 min (Figure 5C). There was no significant difference between 30 and 150 min of pre-incubation, but there was a trend suggesting that 150 min might lead to a greater effect of BTAO. Also, a pre-incubation of 30 min followed by 60 min of experiment time (30/60) showed a similar, non-significant decrease in uptake compared to the 150 min of pre-incubation (Figure 5C). Therefore, we concluded that the optimal pre-incubation time for the inhibitors was 150 min.

To determine which apical channel(s) and/or transporter(s) were responsible for the ^{22}Na uptake, the individual effects of the inhibitors were determined (Figure 5D). As seen in previous experiments (Figure 5C), CD-enriched mouse tubuloid monolayers showed



physiological uptake of ²²Na which was significantly inhibited by BTAO. In addition, the individual effects of the inhibitors clearly showed that this uptake was directly mediated by the amiloride-sensitive ENaC as ²²Na uptake was significantly reduced after inhibition of ENaC with amiloride, with a similar, non-significant reduction compared to the condition with all inhibitors (BTAO). This demonstrates that the ²²Na uptake in the tubuloids was significantly mediated by ENaC. We were not able to detect a significant reduction in ²²Na uptake by inhibition of NKCC2 and NCC alone, which is in line with expression data of these electrolyte transporters.

Discussion

Our current knowledge of kidney (patho)physiology is mainly derived from conventional research models that remain insufficient to fully elucidate certain mechanisms of kidney (patho)physiology (Jung and Kwon, 2016; Edwards and Crambert, 2017; Kleyman and Eaton, 2019). And even though many models have been described, they often lack endogenous expression of relevant ion channels and transporters that are subject to physiological regulation (Yang et al., 2022). Therefore, we have created tubuloids derived from mouse kidney tissue that are differentiated

towards the CD, show physiological channel regulation and functional ion uptake. Previous studies have shown that human tubuloids can be stimulated to increasingly express physiological relevant proteins of certain nephron segment(s) in response to (bio)mechanical and (bio)chemical cues or the lack thereof (e.g., growth factor withdrawal) (Schutgens et al., 2019). We have utilized this plasticity of tubuloids and developed a CD medium that resulted in a remarkable increase of CD proteins that are essential for kidney function (i.e., AQP2 and ENaC), thereby enriching this mouse tubuloid culture for the CD. More specifically, the upregulation of ENaC combined with a lack of enrichment of calbindin D-28K, expressed in the CCD, and UT-A, expressed in the IMCD, suggests that our culture most likely represents the OMCD (Chen et al., 2021). Further characterization of this tubuloid OMCD representation is required to determine protein expression and localization. The upregulation of ENaC in the mouse tubuloid culture on protein level was modest compared to AQP2, which might be explained by the presence of insulin in the medium (a component of advanced DMEM/F12), which is known to indirectly stimulate ENaC expression (Tiwari et al., 2007). We did observe a reduction in the number of additional bands on the alpha ENaC Western blot upon CD-enrichment. This might suggest increased maturity of ENaC since the mouse kidney control showed a similar profile. Also, the presence of alpha ENaC fragments >70–80 kDa in mouse tissue has been shown before by multiple groups (Zhang et al., 2016; Frindt et al., 2020; Bohnert et al., 2021; Artunc et al., 2022). The translocation of AQP2 to the apical membrane of the tubuloids indicates a physiological response to the CD medium component forskolin, which mimics the effect of AVP by raising intracellular cyclic adenosine monophosphate (cAMP) levels (Seamon et al., 1981; Rice et al., 2012). This activates protein kinase A (PKA) which phosphorylates AQP2, thereby triggering its trafficking to the apical membrane (Olesen and Fenton, 2017). Tubuloids also showed a physiological response to stimulation with DDAVP, a synthetic variant of AVP, by upregulation of CD markers and translocation of AQP2 to the apical membrane. This confirms the presence of a functional V2R and associated signalling pathways in mouse tubuloids. For functional studies, ENaC expression and activity was further stimulated by fludrocortisone, an aldosterone analogue and mineralocorticoid agonist (Yamamoto et al., 2016). The CD-enriched mouse tubuloids were capable of amiloride sensitive Na⁺ uptake, demonstrating ENaC-specific Na⁺ transport. Therefore, the presented mouse tubuloids allow to easily isolate epithelial cells that are expandable while maintaining a physiological expression profile and function.

A major advantage of mouse tubuloids is that they can be easily derived from existing (diseased) mouse models for complementary *in vitro* studies while simultaneously reducing the need for additional animal experiments. Our CD differentiation protocol with innate tubuloid AQP2 and ENaC expression and function is of added value for future studies of CD function and regulation. This also includes pathogenic phenotypes (e.g., NDI and Liddle syndrome) that arise from this segment. For example, tubuloids can be obtained from existing mouse (knockout or mutation) models of the V2R, AQP2, and ENaC, thereby providing a model for e.g. hereditary NDI and Liddle's syndrome. Although the molecular mechanisms of Liddle syndrome are well-studied and amiloride is used as an effective therapy against the significant hypertension that many patients suffer from, it has been found that not all patients respond the same way to this therapy which leaves them susceptible for hypertension-induced risks (Pradervand et al., 1999). NDI is a more prevalent disease and novel mutations have been discovered recently (Gao et al., 2020; Li et al., 2021). However, these studies

suggest that some mechanisms of, e.g., AQP2 trafficking remain to be unveiled (Olesen and Fenton, 2021). Because these diseases have low prevalence, patient sample size and lack of clinical data are limitations to further unveil the pathophysiology and improved (personalized) treatments (Enslow et al., 2019; Fan et al., 2020). Here, tubuloids from existing mouse models can be of added value to study these tubulopathies.

Limitations of this study include the heterogeneity of the tubuloid culture and the lack of IC enrichment. Although the CD medium significantly upregulates CD specific proteins, other segments remain present in the culture. Whereas this can be considered as an advantage over single cell type cultures, it can be a disadvantage for some applications. For example, our uptake experiment did not completely diminish the Na⁺ uptake after ENaC inhibition with amiloride. This indicates that the CD-enriched tubuloid culture might still express Na⁺ transporters of other nephron segments. As such, human tubuloids have been shown to express multiple proximal tubule markers, suggesting a large presence of this segment in the culture (Schutgens et al., 2019). For applications that require a homogenic CD culture, cell sorting methods and/or creation of CD reporter lines should be investigated. Examples include growing tubuloids from existing mouse strains with fluorescent-labeled reporter lines for more convenient sorting (Zharkikh et al., 2002; Miller et al., 2006). In addition to the heterogeneity of the culture, we also observed differences in the magnitude of effect between the two tubuloid lines. This suggests that interindividual differences might also play a role in the maturity/functionality. Future studies should further explore the importance of this effect in the CD-enriched tubuloid culture. Furthermore, the CD differentiation medium does not seem to increase expression of ICs. Similar to our results, Shi et al. (2022) recently showed an absence of ICs in their original organoid culture, which could be restored by overexpression of the transcription factor FOXI1. For applications that require ICs, the expression of ICs in the CD-enriched tubuloid culture should be further investigated and the culture procedure might be adapted to increase expression of FOXI1 or other IC transcription factors.

We believe that our CD-enriched tubuloid culture is a unique tool to study CD (patho)physiology. Tubuloids allow for easy accessibility for functional studies, are versatile and easily usable. Our culture system can be used complimentary to iPSC-derived organoids that mimic nephrogenesis. Although these organoids include multiple cell types including stromal and vascular cells, they lack a mature expression profile (Wu et al., 2018). Presence of these cell types increases similarities with the *in vivo* situation, but it also increases complexity for certain experiments. For example, the access to certain cells or specifically the apical compartment is more difficult and the multiple cell types that are present can interfere with the readout. Recent studies have shown efforts to obtain specifically kidney epithelial cells from organoids by either more directed differentiation or isolation of epithelial cells (Montalbetti et al., 2022; Shi et al., 2022). These approaches have enabled functional characterization, including amiloride-sensitive ENaC activity specific to the collecting duct, which would have not been feasible with original organoid protocols. These are valuable developments in the field that allow for functional studies. In this regard, the purely epithelial nature of tubuloids allow for different studies of specific effects on the epithelial cells alone without the interference of other cell types.

In addition to the (bio)chemical cues that can stimulate the expression of certain markers in the tubuloid culture, mechanical cues are also essential. A tubuloid-on-a-chip has been described by Gijzen et al. (2021) which kept the 3D environment of the tubuloids while allowing access to both apical and basolateral sides and applying shear stress. Since the *in vivo* tubular lumen is subjected to shear stress

due to the flow of pre-urine, enabling flow *in vitro* will allow for a more physiological experimental set-up. This is also the case specifically for AQP2 and ENaC, as both channels have been known to be regulated by (bio)mechanical cues including shear stress (Jang et al., 2011; Shi et al., 2013; Cosgun et al., 2022). In this regard, incorporating mouse tubuloids into an organ-on-a-chip system can increase the translational value in future studies.

In conclusion, this study presents a new mouse kidney tubuloid model that can be differentiated towards the CD. CD-enriched mouse tubuloids form a polarized epithelium in 3D that consists of a single epithelial cell layer. This tubuloid culture expresses key channels and transporters of the CD in a polarized fashion and demonstrates CD-specific channel regulation and electrolyte uptake. Therefore, mouse kidney tubuloids allow for future studies of CD physiology and may help to further improve our knowledge of kidney physiology and pathophysiology of (rare) diseases.

Data availability statement

The raw data supporting the conclusion of this article will be made available by the authors, without undue reservation.

Ethics statement

Ethical review and approval was not required for the animal study because the animal procedures were performed in accordance with the guidelines of the Animal Ethics Board of the Radboud University Nijmegen. No specific approval was required for this study, since only surplus animals were used.

Author contributions

CO and ED wrote the manuscript with input from the other authors. MR, IO, MV, and JH conceptualized and supervised the project, designed experiments and performed data analysis and interpretation. CO and ED designed, performed the experiments,

References

- Adams, D. C., Karolak, M. J., Larman, B. W., Liaw, L., Nolin, J. D., and Oxburgh, L. (2010). Follistatin-like 1 regulates renal IL-1 β expression in cisplatin nephrotoxicity. *Am. J. Physiol. Ren. Physiol.* 299 (6), F1320–F1327. doi:10.1152/ajprenal.00325.2010
- Alpern, R. J., and Hebert, S. C. (2007). *Seldin and giebisch's the kidney: Physiology & pathophysiology*, 1-2. Netherland: Elsevier.
- Artunc, F., Bohnert, B. N., Schneider, J. C., Staudner, T., Sure, F., Ilyaskin, A. V., et al. (2022). Proteolytic activation of the epithelial sodium channel (ENaC) by factor VII activating protease (FSAP) and its relevance for sodium retention in nephrotic mice. *Pflügers Archiv - Eur. J. Physiology* 474 (2), 217–229. doi:10.1007/s00424-021-02639-7
- Baer, P. C., Bereiter-Hahn, J., Schubert, R., and Geiger, H. (2006). Differentiation status of human renal proximal and distal tubular epithelial cells *in vitro*: Differential expression of characteristic markers. *Cells Tissues Organs* 184 (1), 16–22. doi:10.1159/000096947
- Bhalla, V., and Hallows, K. R. (2008). Mechanisms of ENaC regulation and clinical implications. *J. Am. Soc. Nephrol.* 19 (10), 1845–1854. doi:10.1681/ASN.2008020225
- Bohnert, B. N., Essigke, D., Janessa, A., Schneider, J. C., Wörn, M., Kalo, M. Z., et al. (2021). Experimental nephrotic syndrome leads to proteolytic activation of the epithelial Na⁺ channel in the mouse kidney. *Am. J. Physiology-Renal Physiology* 321 (4), F480–F493. doi:10.1152/ajprenal.00199.2021
- Brown, D. (2003). The ins and outs of aquaporin-2 trafficking. *Am. J. Physiology-Renal Physiology* 284 (5), F893–F901. doi:10.1152/ajprenal.00387.2002
- Calandrini, C., Schutgens, F., Oka, R., Margaritis, T., Candelli, T., Mathijssen, L., et al. (2020). An organoid biobank for childhood kidney cancers that captures disease and tissue heterogeneity. *Nat. Commun.* 11 (1), 1310. doi:10.1038/s41467-020-15155-6
- Campbell, H. K., Maiers, J. L., and DeMali, K. A. (2017). Interplay between tight junctions & adherens junctions. *Exp. Cell Res.* 358 (1), 39–44. doi:10.1016/j.yexcr.2017.03.061
- Canessa, C. M., Schild, L., Buell, G., Thorens, B., Gautschi, I., Horisberger, J.-D., et al. (1994). Amiloride-sensitive epithelial Na⁺ channel is made of three homologous subunits. *Nature* 367 (6462), 463–467. doi:10.1038/367463a0
- Chen, L., Chou, C. L., and Knepper, M. A. (2021). A comprehensive map of mRNAs and their isoforms across all 14 renal tubule segments of mouse. *J. Am. Soc. Nephrol.* 32 (4), 897–912. doi:10.1681/ASN.2020101406
- Clevers, H. (2016). Modeling development and disease with organoids. *Cell* 165 (7), 1586–1597. doi:10.1016/j.cell.2016.05.082
- Combes, A. N., Zappia, L., Er, P. X., Oshlack, A., and Little, M. H. (2019). Single-cell analysis reveals congruence between kidney organoids and human fetal kidney. *Genome Med.* 11 (1), 3. doi:10.1186/s13073-019-0615-0
- Cosgun, Z. C., Sternak, M., Fels, B., Bar, A., Kwiatkowski, G., Pacia, M. Z., et al. (2022). Rapid shear stress-dependent ENaC membrane insertion is mediated by the endothelial glycocalyx and the mineralocorticoid receptor. *Cell. Mol. Life Sci.* 79 (5), 235. doi:10.1007/s00018-022-04260-y

data analysis and interpretation. FL, JS, and LH performed experiments and contributed to experimental design and interpretation. FY, CA, and JJ contributed to experimental design, planning, interpretation and provided intellectual support.

Acknowledgments

The authors acknowledge the support of the Dutch Kidney Foundation (17PhD04 and 19OK005), the partners of “Regenerative Medicine Crossing Borders” (RegMed XB), Powered by Health~Holland, Top Sector Life Sciences and Health and the Gravitation Program “Materials Driven Regeneration,” funded by the Netherlands Organization for Scientific Research (024.003.013) and the Netherlands Organization for Scientific Research (NWO Veni Grant No: 091 501 61 81 01 36). The authors thank Prof. Koenderink for providing the Na⁺/K⁺-ATPase antibody and C. Bos (Department of Physiology, Radboud University Medical Center, Nijmegen, the Netherlands) for preparing the immunohistochemistry samples. The authors also would like to thank the Radboudumc Technology Center microscopy for their support. Finally, the isotope used in this research was supplied by the U.S. Department of Energy Isotope Program, managed by the Office of Isotope R&D and Production.

Conflict of interest

The authors declare that the research was conducted in the absence of any commercial or financial relationships that could be construed as a potential conflict of interest.

Publisher's note

All claims expressed in this article are solely those of the authors and do not necessarily represent those of their affiliated organizations, or those of the publisher, the editors and the reviewers. Any product that may be evaluated in this article, or claim that may be made by its manufacturer, is not guaranteed or endorsed by the publisher.

- Deen, P. M., Verdijk, M. A., Knoers, N. V., Wieringa, B., Monnens, L. A., van Os, C. H., et al. (1994). Requirement of human renal water channel aquaporin-2 for vasopressin-dependent concentration of urine. *Science* 264 (5155), 92–95. doi:10.1126/science.8140421
- Degirmenci, U., Wang, M., and Hu, J. (2020). Targeting aberrant RAS/RAF/MEK/ERK signaling for cancer therapy. *Cells* 9 (1), 198. doi:10.3390/cells9010198
- Doucet, A. (1988). Function and control of Na-K-ATPase in single nephron segments of the mammalian kidney. *Kidney Int.* 34 (6), 749–760. doi:10.1038/ki.1988.245
- Downie, M. L., Lopez Garcia, S. C., Kleta, R., and Bockenbauer, D. (2021). Inherited tubulopathies of the kidney: Insights from genetics. *Clin. J. Am. Soc. Nephrol.* 16 (4), 620–630. doi:10.2215/CJN.14481119
- Edwards, A., and Crambert, G. (2017). Versatility of NaCl transport mechanisms in the cortical collecting duct. *Am. J. Physiology-Renal Physiology* 313 (6), F1254–F63. doi:10.1152/ajprenal.00369.2017
- Enslow, B. T., Stockand, J. D., and Berman, J. M. (2019). Liddle's syndrome mechanisms, diagnosis and management. *Integr. Blood Press Control* 12, 13–22. doi:10.2147/IBPC.S188869
- Fan, P., Pan, X.-C., Zhang, D., Yang, K.-Q., Zhang, Y., Tian, T., et al. (2020). Pediatric Liddle syndrome caused by a novel SCNN1G variant in a Chinese family and characterized by early-onset hypertension. *Am. J. Hypertens.* 33 (7), 670–675. doi:10.1093/ajh/hpaa037
- Frindt, G., Bertog, M., Korbmayer, C., and Palmer, L. G. (2020). Ubiquitination of renal ENaC subunits in vivo. *Am. J. Physiology-Renal Physiology* 318 (5), F1113–F21. doi:10.1152/ajprenal.00609.2019
- Fushimi, K., Uchida, S., Harat, Y., Hirata, Y., Marumo, F., and Sasaki, S. (1993). Cloning and expression of apical membrane water channel of rat kidney collecting tubule. *Nature* 361 (6412), 549–552. doi:10.1038/361549a0
- Gao, C., Higgins, P. J., and Zhang, W. (2020). AQP2: Mutations associated with congenital nephrogenic diabetes insipidus and regulation by post-translational modifications and protein-protein interactions. *Cells* 9 (10), 2172. doi:10.3390/cells9102172
- Gartzke, D., and Fricker, G. (2014). Establishment of optimized MDCK cell lines for reliable efflux transport studies. *J. Pharm. Sci.* 103 (4), 1298–1304. doi:10.1002/jps.23901
- Geller, D. S., Zhang, J., Zennaro, M.-C., Vallo-Boado, A., Rodriguez-Soriano, J., Furu, L., et al. (2006). Autosomal dominant pseudohypoaldosteronism type 1: Mechanisms, evidence for neonatal lethality, and phenotypic expression in adults. *J. Am. Soc. Nephrol.* 17 (5), 1429–1436. doi:10.1681/ASN.2005111188
- Gijzen, L., Yousef Yengej, F. A., Schutgens, F., Vormann, M. K., Ammerlaan, C. M. E., Nicolas, A., et al. (2021). Culture and analysis of kidney tubuloids and perfused tubuloid cells-on-a-chip. *Nat. Protoc.* 16 (4), 2023–2050. doi:10.1038/s41596-020-00479-w
- Hasler, U., Mordasini, D., Bens, M., Bianchi, M., Cluzeaud, F., Rousselot, M., et al. (2002). Long term regulation of aquaporin-2 expression in vasopressin-responsive renal collecting duct principal cells. *J. Biol. Chem.* 277 (12), 10379–10386. doi:10.1074/jbc.M111880200
- Ishibashi, K., Sasaki, S., Fushimi, K., Uchida, S., Kuwahara, M., Saito, H., et al. (1994). Molecular cloning and expression of a member of the aquaporin family with permeability to glycerol and urea in addition to water expressed at the basolateral membrane of kidney collecting duct cells. *Proc. Natl. Acad. Sci.* 91 (14), 6269–6273. doi:10.1073/pnas.91.14.6269
- Jang, K. J., Cho, H. S., Kang, D. H., Bae, W. G., Kwon, T. H., and Suh, K. Y. (2011). Fluid-shear-stress-induced translocation of aquaporin-2 and reorganization of actin cytoskeleton in renal tubular epithelial cells. *Integr. Biol. (Camb)* 3 (2), 134–141. doi:10.1039/c0ib00018c
- Jenkinson, S. E., Chung, G. W., Van Loon, E., Bakar, N. S., Dalzell, A. M., and Brown, C. D. (2012). The limitations of renal epithelial cell line HK-2 as a model of drug transporter expression and function in the proximal tubule. *Pflügers Archiv-European J. Physiology* 464 (6), 601–611. doi:10.1007/s00424-012-1163-2
- Jensen, C., and Teng, Y. (2020). Is it time to start transitioning from 2D to 3D cell culture? *Front. Mol. Biosci.* 7 (33), 33. doi:10.3389/fmolb.2020.00033
- Jung, H. J., and Kwon, T.-H. (2016). Molecular mechanisms regulating aquaporin-2 in kidney collecting duct. *Am. J. Physiology-Renal Physiology* 311 (6), F1318–F28. doi:10.1152/ajprenal.00485.2016
- Jung, H. J., and Kwon, T.-H. (2019). New insights into the transcriptional regulation of aquaporin-2 and the treatment of X-linked hereditary nephrogenic diabetes insipidus. *Kidney Res. Clin. Pract.* 38 (2), 145–158. doi:10.23876/j.krcp.19.002
- Kavanagh, C., and Uy, N. S. (2019). Nephrogenic diabetes insipidus. *Pediatr. Clin. North Am.* 66 (1), 227–234. doi:10.1016/j.pcl.2018.09.006
- Kleyman, T. R., and Eaton, D. C. (2019). Regulating ENaC's gate. *Am. J. Physiology-Cell Physiology* 318 (1), C150–C62. doi:10.1152/ajpcell.00418.2019
- Koenderink, J. B., Geibel, S., Grabsch, E., De Pont, J. J. H. M., Bamberg, E., and Friedrich, T. (2003). Electrophysiological analysis of the mutated Na, K-ATPase cation binding pocket. *J. Biol. Chem.* 278 (51), 51213–51222. doi:10.1074/jbc.M306384200
- Kohno, M., and Pouyssegur, J. (2006). Targeting the ERK signaling pathway in cancer therapy. *Ann. Med.* 38 (3), 200–211. doi:10.1080/07853890600551037
- Labarca, M., Nizar, J. M., Walczak, E. M., Dong, W., Pao, A. C., and Bhalla, V. (2015). Harvest and primary culture of the murine aldosterone-sensitive distal nephron. *Am. J. Physiology Ren. physiology* 308 (11), F1306–F1315. doi:10.1152/ajprenal.00668.2014
- Li, Q., Tian, D., Cen, J., Duan, L., and Xia, W. (2021). Novel AQP2 mutations and clinical characteristics in seven Chinese families with congenital nephrogenic diabetes insipidus. *Front. Endocrinol.* 12, 686818. doi:10.3389/fendo.2021.686818
- Maric, K., Oksche, A., and Rosenthal, W. (1998). Aquaporin-2 expression in primary cultured rat inner medullary collecting duct cells. *Am. J. Physiology-Renal Physiology* 275 (5), F796–F801. doi:10.1152/ajprenal.1998.275.5.F796
- Masilamani, S., Kim, G. H., Mitchell, C., Wade, J. B., and Knepper, M. A. (1999). Aldosterone-mediated regulation of ENaC alpha, beta, and gamma subunit proteins in rat kidney. *J. Clin. Invest.* 104 (7), R19–R23. doi:10.1172/JCI7840
- Miller, R. L., Zhang, P., Chen, T., Rohrwasser, A., and Nelson, R. D. (2006). Automated method for the isolation of collecting ducts. *Am. J. Physiology-Renal Physiology* 291 (1), F236–F245. doi:10.1152/ajprenal.00273.2005
- Montalbetti, N., Przepiorski, A. J., Shi, S., Sheng, S., Baty, C. J., Maggiore, J. C., et al. (2022). Functional characterization of ion channels expressed in kidney organoids derived from human induced pluripotent stem cells. *Am. J. Physiology-Renal Physiology* 323 (4), F479–F491. doi:10.1152/ajprenal.00365.2021
- Nielsen, S., Chou, C. L., Marples, D., Christensen, E. I., Kishore, B. K., and Knepper, M. A. (1995). Vasopressin increases water permeability of kidney collecting duct by inducing translocation of aquaporin-CD water channels to plasma membrane. *Proc. Natl. Acad. Sci. U. S. A.* 92 (4), 1013–1017. doi:10.1073/pnas.92.4.1013
- Olesen, E. T. B., and Fenton, R. A. (2017). Aquaporin-2 membrane targeting: Still a conundrum. *Am. J. Physiology-Renal Physiology* 312 (4), F744–F7. doi:10.1152/ajprenal.00101.2017
- Olesen, E. T. B., and Fenton, R. A. (2021). Aquaporin 2 regulation: Implications for water balance and polycystic kidney diseases. *Nat. Rev. Nephrol.* 17 (11), 765–781. doi:10.1038/s41581-021-00447-x
- Poladia, D. P., Kish, K., Kutay, B., Hains, D., Kegg, H., Zhao, H., et al. (2006). Role of fibroblast growth factor receptors 1 and 2 in the metanephric mesenchyme. *Dev. Biol.* 291 (2), 325–339. doi:10.1016/j.ydbio.2005.12.034
- Pradervand, S., Wang, Q., Burnier, M., Beermann, F., Horisberger, J. D., Hummler, E., et al. (1999). A mouse model for liddle's syndrome. *J. Am. Soc. Nephrol.* 10, 2527.
- Preibisch, S., Saalfeld, S., and Tomancak, P. (2009). Globally optimal stitching of tiled 3D microscopic image acquisitions. *Bioinformatics* 25 (11), 1463–1465. doi:10.1093/bioinformatics/btp184
- Ramboer, E., De Craene, B., De Kock, J., Vanhaecke, T., Bex, G., Rogiers, V., et al. (2014). Strategies for immortalization of primary hepatocytes. *J. Hepatology* 61 (4), 925–943. doi:10.1016/j.jhep.2014.05.046
- Rice, W. L., Zhang, Y., Chen, Y., Matsuzaki, T., Brown, D., and Lu, H. A. (2012). Differential, phosphorylation dependent trafficking of AQP2 in LLC-PK1 cells. *PLoS One* 7 (2), e32843. doi:10.1371/journal.pone.0032843
- Russell, W. M. S., and Burch, R. L. (1959). *The principles of humane experimental technique*. London: Methuen and Co limited.
- Sandoval, P. C., Slentz, D. H., Pisitkun, T., Saeed, F., Hoffert, J. D., and Knepper, M. A. (2013). Proteome-wide measurement of protein half-lives and translation rates in vasopressin-sensitive collecting duct cells. *J. Am. Soc. Nephrol.* 24 (11), 1793–1805. doi:10.1681/ASN.2013030279
- Schindelin, J., Arganda-Carreras, I., Frise, E., Kaynig, V., Longair, M., Pietzsch, T., et al. (2012). Fiji: An open-source platform for biological-image analysis. *Nat. Methods* 9 (7), 676–682. doi:10.1038/nmeth.2019
- Schutgens, F., Rookmaaker, M. B., Margaritis, T., Rios, A., Ammerlaan, C., Jansen, J., et al. (2019). Tubuloids derived from human adult kidney and urine for personalized disease modeling. *Nat. Biotechnol.* 37 (3), 303–313. doi:10.1038/s41587-019-0048-8
- Schutgens, F., Rookmaaker, M., and Verhaar, M. (2021). A perspective on a urine-derived kidney tubuloid biobank from patients with hereditary tubulopathies. *Tissue Eng. Part C Methods* 27 (3), 177–182. doi:10.1089/ten.TEC.2020.0366
- Seamon, K. B., Padgett, W., and Daly, J. W. (1981). Forskolin: Unique diterpene activator of adenylate cyclase in membranes and in intact cells. *Proc. Natl. Acad. Sci. U. S. A.* 78 (6), 3363–3367. doi:10.1073/pnas.78.6.3363
- Shi, S., Carattino, M. D., Hughey, R. P., and Kleyman, T. R. (2013). ENaC regulation by proteases and shear stress. *Curr. Mol. Pharmacol.* 6 (1), 28–34. doi:10.2174/18744672112059990027
- Shi, M., McCracken, K. W., Patel, A. B., Zhang, W., Ester, L., Valerius, M. T., et al. (2022). Human uterine bud organoids recapitulate branching morphogenesis and differentiate into functional collecting duct cell types. *Nat. Biotechnol.* doi:10.1038/s41587-022-01429-5
- Slusser, A., Bathula, C. S., Sens, D. A., Somji, S., Sens, M. A., Zhou, X. D., et al. (2015). Cadherin expression, vectorial active transport, and metallothionein isoform 3 mediated EMT/MET responses in cultured primary and immortalized human proximal tubule cells. *PLoS One* 10 (3), e0120132. doi:10.1371/journal.pone.0120132
- Takasato, M., Er, P. X., Chiu, H. S., Maier, B., Baillie, G. J., Ferguson, C., et al. (2015). Kidney organoids from human iPSCs contain multiple lineages and model human nephrogenesis. *Nature* 526 (7574), 564–568. doi:10.1038/nature15695
- Terris, J., Ecelbarger, C. A., Marples, D., Knepper, M., and Nielsen, S. (1995). Distribution of aquaporin-4 water channel expression within rat kidney. *Am. J. Physiology-Renal Physiology* 269 (6), F775–F785. doi:10.1152/ajprenal.1995.269.6.F775
- Terry, S., Jouret, F., Vandenabeele, F., Smolders, I., Moreels, M., Devuyt, O., et al. (2007). A primary culture of mouse proximal tubular cells, established on collagen-coated membranes. *Am. J. Physiol. Ren. Physiol.* 293 (2), F476–F485. doi:10.1152/ajprenal.00363.2006

- Tiwari, S., Nordquist, L., Halagappa, V. K., and Ecelbarger, C. A. (2007). Trafficking of ENaC subunits in response to acute insulin in mouse kidney. *Am. J. Physiol. Ren. Physiol.* 293 (1), F178–F185. doi:10.1152/ajprenal.00447.2006
- Tojo, M., Hamashima, Y., Hanyu, A., Kajimoto, T., Saitoh, M., Miyazono, K., et al. (2005). The ALK-5 inhibitor A-83-01 inhibits Smad signaling and epithelial-to-mesenchymal transition by transforming growth factor-beta. *Cancer Sci.* 96 (11), 791–800. doi:10.1111/j.1349-7006.2005.00103.x
- Ufer, E., Postina, R., Gorbulev, V., and Fahrenholz, F. (1995). An extracellular residue determines the agonist specificity of V2 vasopressin receptors. *FEBS Lett.* 362 (1), 19–23. doi:10.1016/0014-5793(95)00150-8
- van Balkom, B. W., van Raak, M., Breton, S., Pastor-Soler, N., Bouley, R., van der Sluijs, P., et al. (2003). Hypertonicity is involved in redirecting the aquaporin-2 water channel into the basolateral, instead of the apical, plasma membrane of renal epithelial cells. *J. Biol. Chem.* 278 (2), 1101–1107. doi:10.1074/jbc.M207339200
- Van der Hauwaert, C., Savary, G., Gnemmi, V., Glowacki, F., Pottier, N., Bouillez, A., et al. (2013). Isolation and characterization of a primary proximal tubular epithelial cell model from human kidney by CD10/CD13 double labeling. *PLoS one* 8 (6), e66750. doi:10.1371/journal.pone.0066750
- Van der Hauwaert, C., Savary, G., Buob, D., Leroy, X., Aubert, S., Flamand, V., et al. (2014). Expression profiles of genes involved in xenobiotic metabolism and disposition in human renal tissues and renal cell models. *Toxicol. Appl. Pharmacol.* 279 (3), 409–418. doi:10.1016/j.taap.2014.07.007
- van Lieburg, A. F., Knoers, N. V., and Deen, P. M. (1995). Discovery of aquaporins: A breakthrough in research on renal water transport. *Pediatr. Nephrol.* 9 (2), 228–234. doi:10.1007/BF00860757
- Watanabe, K., Ueno, M., Kamiya, D., Nishiyama, A., Matsumura, M., Wataya, T., et al. (2007). A ROCK inhibitor permits survival of dissociated human embryonic stem cells. *Nat. Biotechnol.* 25 (6), 681–686. doi:10.1038/nbt1310
- Wiraja, C., Mori, Y., Ichimura, T., Hwang, J., Xu, C., and Bonventre, J. V. (2021). Nephrotoxicity assessment with human kidney tubuloids using spherical nucleic acid-based mRNA nanoflares. *Nano Lett.* 21 (13), 5850–5858. doi:10.1021/acs.nanolett.1c01840
- Wu, H., Uchimura, K., Donnelly, E. L., Kirita, Y., Morris, S. A., and Humphreys, B. D. (2018). Comparative analysis and refinement of human PSC-derived kidney organoid differentiation with single-cell transcriptomics. *Cell Stem Cell* 23 (6), 869–881. doi:10.1016/j.stem.2018.10.010
- Yamamoto, T., Sasaki, S., Fushimi, K., Ishibashi, K., Yaoita, E., Kawasaki, K., et al. (1995). Vasopressin increases AQP-CD water channel in apical membrane of collecting duct cells in Brattleboro rats. *Am. J. Physiol.* 268, C1546–C1551. doi:10.1152/ajpcell.1995.268.6.C1546
- Yamamoto, S., Hotta, Y., Maeda, K., Kataoka, T., Maeda, Y., Hamakawa, T., et al. (2016). Mineralocorticoid receptor stimulation induces urinary storage dysfunction via upregulation of epithelial sodium channel expression in the rat urinary bladder epithelium. *J. Pharmacol. Sci.* 130 (4), 219–225. doi:10.1016/j.jphs.2016.02.004
- Yang, H-H., Su, S-H., Ho, C-H., Yeh, A-H., Lin, Y-J., and Yu, M-J. (2022). Glucocorticoid receptor maintains vasopressin responses in kidney collecting duct cells. *Front. Physiol.* 13, 816959. doi:10.3389/fphys.2022.816959
- Yu, X., Chen, L., Wu, K., Yan, S., Zhang, R., Zhao, C., et al. (2018). Establishment and functional characterization of the reversibly immortalized mouse glomerular podocytes (imPODs). *Genes & Dis.* 5 (2), 137–149. doi:10.1016/j.gendis.2018.04.003
- Zhang, C., Wang, L., Su, X-T., Zhang, J., Lin, D-H., and Wang, W-H. (2016). ENaC and ROMK activity are inhibited in the DCT2/CNT of TgWnk4PHAI mice. *Am. J. Physiology-Renal Physiology* 312 (4), F682–F8. doi:10.1152/ajprenal.00420.2016
- Zharkikh, L., Zhu, X., Stricklett, P. K., Kohan, D. E., Chipman, G., Breton, S., et al. (2002). Renal principal cell-specific expression of green fluorescent protein in transgenic mice. *Am. J. Physiology-Renal Physiology* 283 (6), F1351–F1364. doi:10.1152/ajprenal.0224.2001